Multipath Exploitation and Suppression for SAR Imaging of Building Interiors

Michael Leigsnering, *Student Member, IEEE,* Moeness G. Amin, *Fellow, IEEE,* Fauzia Ahmad, *Senior Member, IEEE,* and Abdelhak M. Zoubir, *Fellow, IEEE*

Abstract

Multipath that involves target scattering is an important phenomenon in synthetic aperture radar (SAR). It is highly pronounced in imaging of building interiors due to the presence of walls, ceilings, and floors surrounding the targets of interest. Multipath attributed to targets is a special type of clutter, which can be either suppressed or exploited. The latter has been the subject of many recent works in the area of SAR imaging and has led to tangible improvements in target detection and localization. In this paper, we consider state-of-the-art multipath suppression and exploitation approaches, present their corresponding analytical models, and highlight their respective requirements, assumptions, and offerings. Both conventional and compressive sensing based approaches are discussed, where the latter assumes the presence of few behind-the-wall targets.

I. Introduction

In recent years, radar imaging of building interiors has gained much interest due to the rising and ubiquitous use in civilian, security, and defense applications [1]–[3]. Typically, there is no visual access to the scene, and optical, ultrasound, or thermal imaging is not effective. In this case, sensing is performed by the electromagnetic (EM) modality and has allowed the emergence of the area of through-the-wall radar imaging (TWRI). Indoor targets and interior building layout are detected and characterized from a standoff distance. The radar systems may be ground-based

M. Leigsnering and A. M. Zoubir are with the Signal Processing Group, Institute of Telecommunications, Technische Universität Darmstadt, 64283 Darmstadt, Germany (e-mail: leigsnering@spg.tu-darmstadt.de; zoubir@spg.tu-darmstadt.de).

F. Ahmad and M. G. Amin are with the Radar Imaging Laboratory, Center for Advanced Communications, Villanova University, Villanova, PA 19085 USA (e-mail: fauzia.ahmad@villavova.edu; moeness.amin@villanova.edu).

or airborne and assume different modes of operations and system parameters. One mode, which is consistent with many sensing objectives, is synthetic aperture radar (SAR). TWRI using SAR is the only viable choice when two-dimensional (2-D) physical apertures required to achieve the desired resolution are logistically difficult or impossible. We restrict the discussions to SAR imaging of stationary targets. Moving targets pose a whole set of different challenges, exceeding the scope of this article.

SAR imaging could be impaired by the many scatterers present in a typical indoor scene. In addition to the shortest path to the target and back to the receiver, the transmitted wave may travel on indirect paths due to secondary reflections arising from interior walls, floor, and ceiling. This leads to rich multipath associated with the targets, which, depending on the scattering environment, can have different adverse effects on the image quality and interpretation. The energy in the multipath returns may accumulate at locations where no physical targets reside, thus creating “ghosts”. With increased specular and diffuse scatterings, the stationary scene can become very cluttered, masking the true targets and disabling their detection. The significance of multipath and ghost targets in imaging of building interiors has been shown in various works. Dogaru and Le [3] showed the ghost phenomenon using extensive numerical EM simulations. Others examined the same, using measurements in a lab setup [4], [5]. The radar community also acknowledged multipath as a significant problem on a special industry day [6].

Since multipath exists and is often observed, it must be described and accounted for, using accurate analytical models, and properly addressed in imaging techniques. Broadly, there are two paradigms to deal with indirect propagation, namely, multipath suppression and multipath exploitation. The key idea of the former is to characterize the multipath returns and mitigate their effects on image formation [7]–[16]. Different properties of direct and indirect radar returns can be used to distinguish between the two arrivals and attenuate, if not remove, the indirect returns. These methods are generally straightforward to apply. However, they do not make use of the energy and target information contained in the multipath returns. The second method, reminiscent of the RAKE receiver in wireless communications [17], aims at exploiting the multipath and using it for imaging enhancements [4], [5], [18]–[24]. By properly modeling the indirect propagation paths, whether they are resolvable or not, their energy can be captured and attributed to their respective targets, allowing an increase in target to clutter and noise ratios, and thus culminating in an enhanced image. Further, areas in the shadow region of highly attenuative targets, which cannot be illuminated by the radar directly, can be imaged by utilizing multipath. Although

multipath exploitation has potential and tangible benefits, it often requires prior information or is computationally demanding.

II. Signal Model

A forward scattering model should be developed in order for multipath to be properly exploited or mitigated. This requires determining the scattered field from the targets inside the building. If the building layout and imaging geometry is known, this problem can be exactly solved by using Maxwell's equations [25]. However, there are two issues that render this approach impractical. First, solving a full wave model is computationally demanding and may require vast resources. Second, inferring the positions of the scatterers from the scattered field, requires solving an inverse problem. Since the forward problem is nonlinear due to the influence of the scatterers on the surrounding field, the inverse problem is even more challenging and, for practical purposes, impossible to solve. In order to overcome these difficulties, various linear approximations of the forward scattering model, such as the Born approximation, Kirchoff approximation, and Geometric Optics (GO), have been introduced, all of which yield tractable solutions to the inverse problem [1], [26], [27]. More specifically, the Born approximation makes the weak scatterer assumption, i.e. the electrical parameters of the scatterers do not differ much from that of the background medium. As such, the total field inside the target is approximated by the incident field [26]. The Kirchhoff or Physical Optics (PO) approximation assumes perfectly conducting targets, and the interaction with the incident field takes place on the surface of the targets only [27]. For both Born and PO approximations, the background medium, which is the building enclosure in the problem at hand, is described by the Green's function that depicts the impulse response of the wave equation. The GO or ray tracing approach uses local plane wave assumption or "ray of light" to model the propagation of the wave [1]. Since the latter is the simplest and most commonly used approximation in TWRI, we focus on ray tracing for describing the signal model.

A. Basic Signal Model

Consider an N-element monostatic linear array of transceivers. Either all of the array elements can be physically present or a single transceiver can be moved to different locations to synthesize the intended aperture. For the synthetic aperture, we assume the stop-and-go approximation for the movement pattern, i.e. the transceiver remains stationary while it transmits and receives at a particular array position and then moves to the next location. The model may be extended to a

bistatic or multi-input multi-output (MIMO) SAR scenario where the transmitter(s) and receiver(s) move along different trajectories. However, this is not treated here for the sake of simplicity.

The linear array is located along the x-axis parallel to an exterior wall of thickness d, with its element locations denoted by $u_n, n = 0, \ldots, N-1$. At the nth array element location, a modulated wideband pulse $\Re\{s(t)\exp(j2\pi f_c t)\}$ is transmitted, where t is the fast time, $s(t)$ is the pulse in the complex baseband, and f_c is the carrier frequency. For a scene of P stationary point targets behind the wall at positions (x_p, z_p), the nth element receives the baseband signal $y_n(t)$, given by

$$y_n(t) = \sum_{p=0}^{P-1} \sigma_p s\left(t - \tau_{pn}\right) \exp\left(-j2\pi f_c \tau_{pn}\right) + v_n(t), \tag{1}$$

where σ_p is the deterministic complex reflectivity of the pth target, and τ_{pn} is the two-way propagation delay between the nth transceiver and the pth target. We consider additive receiver noise $v_n(t)$, which is typically assumed to be i.i.d. complex circular Gaussian process. For through-the-wall propagation, τ_{pn} comprises the components corresponding to traveling distances before, through, and after the wall [1]. Note that the received signal is a superposition of the individual direct target returns only. Target interactions with other targets and the surrounding environment are ignored in this model. However, in indoor scenarios, such interactions are both pronounced and measurable, and give rise to multipath propagation.

B. Multipath Propagation Model

We broadly categorize multipath returns as follows:

- *Interior Wall/Floor/Ceiling Multipath:* These involve indirect paths with secondary specular reflections at a large smooth surface.
- *Wall Ringing Multipath:* This type involves signals that undergo multiple reflections within the exterior wall on transit to/from the targets.
- *Target-to-Target Interaction:* This includes paths where the wave interacts with more than one diffusely scattering targets.

The interior wall/floor/ceiling multipath returns can be further subdivided into the following classes:

- *First order multipath:* This involves one secondary reflection either on transmit or/receive path.
- *Second order multipath:* This involves two secondary reflections during the round-trip path.

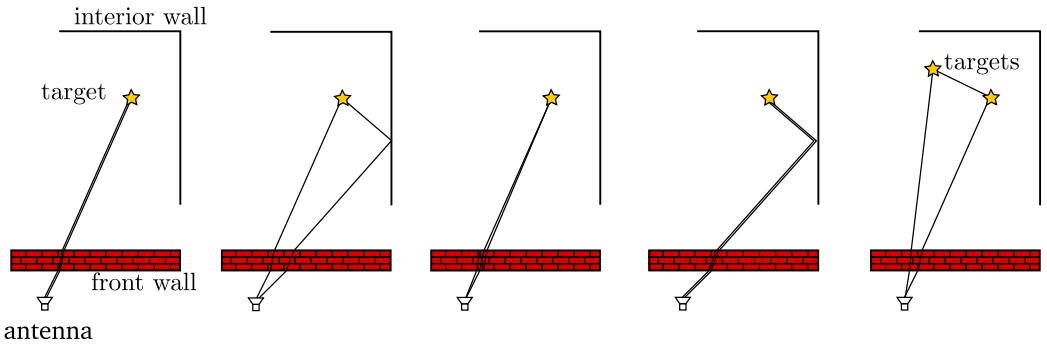

Fig. 1. Various cases for multipath in indoor-scenes. From left to right: direct propagation, one secondary reflection at an interior wall, multiple reflections inside front wall, two secondary reflections at an interior wall, and target-target multipath.

- *Higher-order multipath:* This includes multipath returns involving three or more secondary reflections during the round-trip path.

Fig. 1 shows examples of various multipath propagation cases. As the signal weakens at each secondary reflection, the higher-order multipath returns can usually be neglected.

Considering a maximum of R possible propagation paths for each target-transceiver combination, including the direct path and excluding target-to-target interactions, we can extend the nth received signal model in (1) as

$$y_n(t) = \sum_{r=0}^{R-1} \sum_{p=0}^{P-1} \sigma_p^{(r)} s\left(t - \tau_{pn}^{(r)}\right) \exp\left(-j2\pi f_c \tau_{pn}^{(r)}\right) + v_n(t), \tag{2}$$

where $\tau_{pn}^{(r)}$ is the round-trip propagation delay between the nth transceiver and the pth target along the rth path, and $\sigma_p^{(r)}$ is the complex reflectivity of the pth target when observed through the rth path. Let $r = 0$ correspond to the direct path and the remaining $R - 1$ be the multipath returns. The various propagation delays can be readily calculated using GO considerations [5]. The number paths R is a deterministic parameter that depends on the number and type of scattering walls, which are assumed to be known *a priori*. For illustration, Fig. 2 depicts an example of an interior wall multipath. The associated propagation delay may be determined by considering the equivalent two-way path to the corresponding virtual target. Target-to-target interactions can be included in the multipath model of (2) by assuming additional double bounce paths between pairs of diffusely scattering targets. Note that, in this case, the associated propagation delays not only depend on the distances between the transceivers and the targets, but also on the separation between the targets themselves.

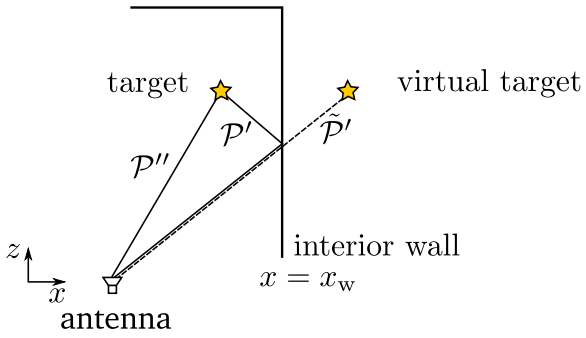

Fig. 2. Multipath propagation via reflection at an interior wall.

C. Image Formation and the Effects of Multipath

Having developed the forward scattering model, we now proceed with the inverse problem of determining the locations of the P point targets. The conventional approach is delay-and-sum beamforming or backprojection, which does not account for multipath propagation. As the number targets is usually unknown *a priori*, the target space is discretized into a rectangular grid of P pixels. Hence, P is the deterministic total number of possible target positions, which is determined by the dimensions of the area being imaged and the system resolution. A non-existing target is simply represented by a pixel with zero reflectivity. An estimate of the image is obtained as [1]

$$I(p) = \frac{1}{N} \sum_{n=0}^{N-1} y_n(t) * s(-t)|_{t=\tau_{pn}^{(0)}}, p = 0, \cdots, P-1, \tag{3}$$

which employs matched filtering of the nth received signal, followed by sampling the output at the delay corresponding to direct propagation to the current pixel, and finally, coherently summing the results corresponding to all N array locations.

If multipath returns are present in the received signals, the image formation process results in ghost targets, i.e., the energy in the multipath returns is focused at locations where no physical targets exist. Fig. 3 shows the image of a scene consisting of two point targets inside a room, which was obtained by applying beamforming to data simulated using (2). In addition to the direct returns, only first-order interior wall multipath and two wall ringing multipath returns per target were assumed to be present in the measurements. We observe that the multipath via reflections at interior walls causes ghosts within the room, whereas the wall ringing multipath creates equally spaced copies of the target response in the downrange direction. The ghosts cause the scene image to be highly cluttered, rendering interpretation difficult and challenging.

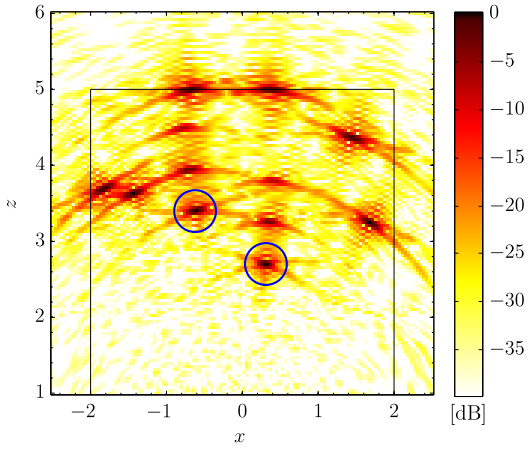

Fig. 3. Beamformed image of a two target scene showing 5 ghost targets associated with each target ($R = 6$ propagation paths per target).

III. Multipath Suppression

Having described the multipath model and the cluttering effects of multipath propagation, we revert back to multipath suppression and exploitation. The objective of multipath suppression is to mitigate the effects of indirect propagation on the quality of the reconstructed scene image. A variety of multipath suppression methods have been devised [7]–[14], which can either act directly on the raw data measurements or are implemented as a post-processing step for the SAR image. These methods require the targets and ghosts/multipath returns to be well resolved and can achieve ghost suppression without any prior knowledge of the scene.

A. Suppression using Ghost Properties in SAR Images

We first describe methods applicable to suppression of ghosts in SAR images resulting from target-to-target interactions. Considering two targets separated by a distance 2δ, the received signal at the nth transceiver location would consist of three components: the two direct returns with respective round-trip propagation delays $\tau_{1n}^{(0)}$ and $\tau_{2n}^{(0)}$, and a double scattering return involving the two targets with a round-trip propagation delay of $\tau_n^{(1)} = \frac{\tau_{1n}^{(0)}+\tau_{2n}^{(0)}}{2} + \frac{2\delta}{c}$, where c is the speed of light in free-space. Since the conventional SAR image formation method, described in Section II-C, is based on direct returns of single target scatterings, the additional delay associated with the double scattering multipath results in a ghost located at a farther range than the two targets, as shown in Fig. 5(a).

Ghosts in SAR images resulting from target-to-target interactions have very specific charac-

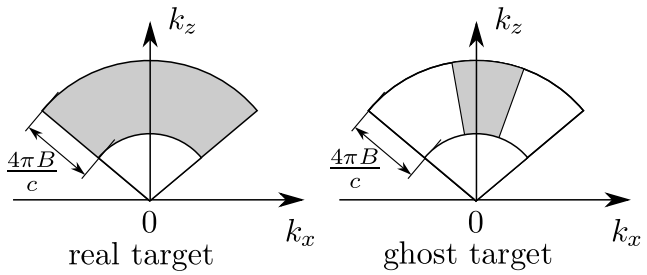

Fig. 4. The support angle of SAR echoes in the wavenumber domain. Ghost target exhibits a narrower support as compared to the real target.

teristics, which can be exploited to distinguish them from real targets. These characteristics stem from the changes in the associated double scattering geometry with aspect angle as viewed by the imaging system [7]. Most targets exhibit aspect dependent scattering. However, unlike the targets, the ghost intensity takes on high values only over a portion of the synthetic aperture (see Fig. 4), implying a smaller effective aperture for imaging of ghosts. This causes a wider point spread function in crossrange for the ghosts as compared to a real target, and subsequently lower crossrange resolution. Second, the phase characteristics of the ghost differ across the SAR aperture, leading to changes in the ghost location when observed through different smaller sub-apertures. This same characteristic causes the ghosts to be defocused when employing the full aperture. In order to reveal the ghost characteristics in SAR images, the full aperture is typically split into small sub-apertures for separate imaging. The above ghost characteristics across the sub-aperture images are effectively used for its suppression.

A simple technique for using the variation of the ghost intensity across the sub-aperture images was proposed in [7]. For each "candidate" target, the variance of the intensity is calculated across the sub-aperture images. Candidates with high variance are identified as ghosts, and are attenuated or suppressed to obtain a ghost-free image. A more sophisticated technique models the intensity variations to distinguish between the targets and the ghosts based on their aspect dependency [8]. However, the target intensity is also a function of its orientation, which is typically unknown. As such, the intensity variation across the various sub-aperture images can be modeled by a hidden Markov model (HMM), where the hidden states are the possible target orientations. The output of the HMM is the intensity profile $\boldsymbol{\rho} \in \mathbb{R}^M$ of a certain image pixel, where M is the number of sub-apertures. Training data from known targets is used to estimate the state-transition probabilities, the probability of observing a certain intensity in a given state, and the initial state

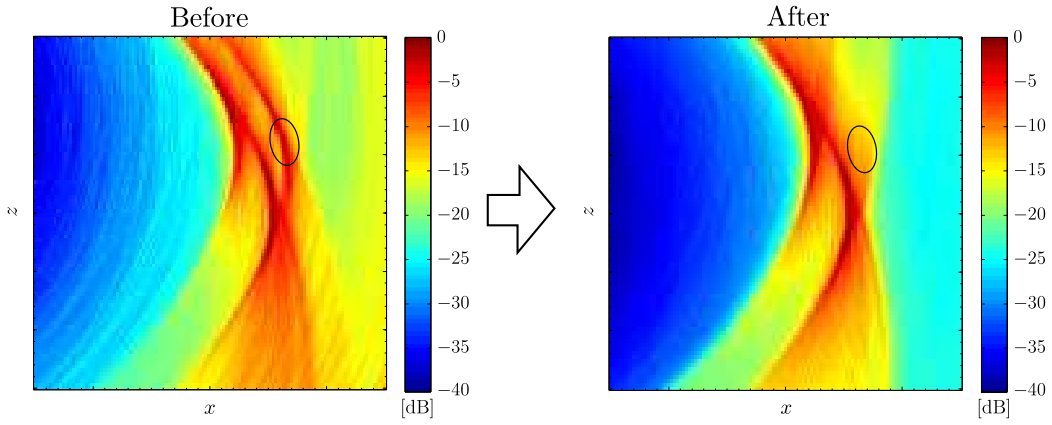

Fig. 5. Multipath suppression using HMM based approach [8]. The ghost at the highlighted position has been suppressed.

probabilities. Thus, a specific HMM can be built for each considered target type. For notational brevity, we consider only one target type, denoted by T_1.

In the testing phase, sub-aperture images are created from the full aperture image using directional filters. The pth image pixel has a corresponding intensity profile $\boldsymbol{\rho}_p$, which may or may not be generated by the T_1 target. The trained HMM is used to evaluate the likelihood that the observed intensity profile is generated by the given target. The likelihood is given by

$$\mathrm{P}(\boldsymbol{\rho}_p|T_1) = \sum_{\text{all } \boldsymbol{q}} \mathrm{P}(\boldsymbol{\rho}_p|\boldsymbol{q}, T_1)\mathrm{P}(\boldsymbol{q}|T_1), \tag{4}$$

where $\mathrm{P}(\boldsymbol{\rho}_p|\boldsymbol{q}, T_1)$ is the probability that $\boldsymbol{\rho}_p$ was generated by state sequence $\boldsymbol{q}$ given target T_1, $\mathrm{P}(\boldsymbol{q}|T_1)$ is the probability that state sequence $\boldsymbol{q}$ occurs given target T_1, and the summation is carried out over all possible state sequences $\boldsymbol{q}$. If the pixel corresponds to the target, the likelihood should be high, whereas the value should be low if it corresponds to a multipath ghost. The pixel in the ghost-mitigated image is obtained by multiplying the original full aperture image pixel with the obtained likelihood value,

$$I(p)^{\text{mitigated}} = \mathrm{P}(\boldsymbol{\rho}_p|T_1)I(p).$$

Hence, only targets that fit the considered model with a high likelihood are retained and the ghosts are suppressed. The performance of the approach is illustrated in Fig. 5. The ghost is strongly visible in the original image. However, it has been suppressed by about 15 dB in the processed image.

A different class of algorithms exploits the differences in the phase history of the sub-aperture

images [9]. As explained above, the ghost targets exhibit a different phase history when viewed from different aspect angles, which depends on the distance 2δ between the two scattering centers. This is exploited for a SAR image reconstruction scheme that generates a separate image for each assumed δ. The true scatterer positions are then contained in the direct path image with $\delta = 0$. This approach can be combined with a scheme that exploits the drift of ghost targets with aspect angle [10]. Drifting and non-drifting target candidates are separated using the Fourier transform of a sub-aperture image pair. Non-drifting targets are retained, whereas drifting targets are suppressed. An issue with the described approach is that the phase changes have to be observed over a large number of aspect angles. Hence, a large aperture and antennas with a large azimuth beamwidth are required. This may work against the power constraints of the transmit chain.

One way to overcome the large synthetic aperture constraint is to exploit the nonlinearity in the phase delays of the ghosts directly in the raw data [11]. Under far-field assumptions, real targets exhibit a linear phase shift when viewed from a shifted aperture. In contrast, the ghosts have an additional nonlinear term in the phase history, which can be exploited to cancel multipath returns and obtain a ghost-free image.

All of the aforementioned methods have been mainly developed under the assumption of far-field conditions, which are mostly applicable to airborne platforms. For ground-based systems, the building resides usually in the near-field, and may be observed from different sides. This gives rise to another approach for ghost suppression in TWRI [12]. An image is generated for each vantage point used to interrogate the building interior. After image registration, the primary reflections, i.e., the true targets, stay at the same location in all images. However, multipath returns place ghosts at different locations, since the multipath reflection geometry changes with the vantage point. Thus, multiplicative fusion of the registered images retains the overlapping true targets and mitigates the non-overlapping ghosts. This approach is conceptually similar to [9], [10]. However, the drifts are much larger as the vantage points have a large separation. We note that, as the secondary specular reflection geometry is a function of the vantage point or aspect angle, the drift-based methods described above are also applicable to specular multipath cases.

B. Other Methods for Multipath Suppression

In this section, we briefly discuss multipath suppression methods that do not fit in the above considered class of algorithms. One possibility is a colocated MIMO based approach [13]. In MIMO radar imaging, orthogonal waveforms are transmitted from a transmit array and the scene

reflections are received, using a receive array. Exploiting the orthogonality of the transmitted waveforms, the returns can be associated with the respective transmitter. From the propagation model, we know that the angle of departure (AOD) equals the angle of arrival (AOA) for the direct path. However, in the multipath propagation case, particularly so for specular multipath, the transmit and receive paths are different and, consequently, the AOA is different from the AOD. This effect can be exploited by using spatial filtering on the transmit and receive signals. By retaining only the signal components with equal AOA and AOD, the multipath returns can be filtered out. Polarimetric features of the secondary reflections have also been exploited for multipath suppression [14]. Double scattering of the wave may change the polarization characteristics, which can be used to differentiate between targets and ghosts. Finally, even an optimized imaging geometry may help reduce ghosting [15]. If the secondary scatterer is known, the SAR trajectory can be adjusted such that very little energy is contained in the multipath returns.

For extended targets modeled by a number of scattering centers, ghosts can appear on or in the vicinity of the back wall due to target obstructing incident waves from reaching the back walls. This presents a vacuum in the image along the back wall or, if change detection is applied, it creates ghosts, which could be stronger than targets. In this case, ghost mitigation can proceed utilizing the respective inter-related geometry of target and ghosts. Extended targets tend, in general, to produce blurred ghosts beyond those created by point target model.

IV. Multipath Exploitation

Multipath suppression discards the energy contained in the multipath returns in order to reduce their adverse effects on the image. Since multipath returns ultimately originate from the target, it is prudent to utilize the energy and information contained in such indirect target returns. Proper exploitation of the multipath returns has been shown to lead to higher signal-to-clutter ratio (SCR), higher crossrange resolution, and extended imaging regions. However, all these imaging enhancements usually come at a price. Multipath exploitation schemes either require prior knowledge of the scattering environment or incur higher computational costs. In the sequel, we categorize multipath exploitation methods according to their multipath resolution requirements.

A. Exploitation Requiring Resolved Multipath

For resolved multipath, the radar returns are well separated in fast time and form the target images and their ghosts. This category includes shadow region imaging in indoor settings [18], where

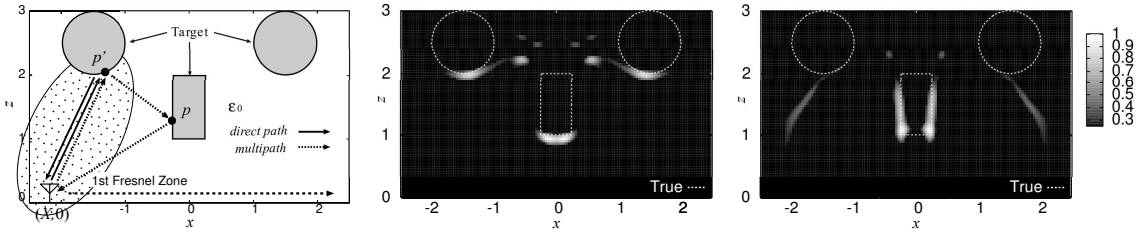

Fig. 6. Propagation paths of single and double scattered waves.

information of hidden areas of spatially extended targets, which are not in the line-of-sight of the radar, is obtained by exploiting target-to-target interactions. The proposed multipath exploitation is a two-step procedure. First, a conventional SAR image $I(\cdot)$ is obtained using the radar returns. The scattering centers observed in the conventional SAR image are treated as new sources for the double scattered multipath returns. That is, the scattering centers act as new transmitters that can illuminate the shadow region of the targets. Next, a modified SAR algorithm is employed that assumes double-scattering propagation to obtain an image $I^{\text{double}}(\cdot)$ as

$$I^{\text{double}}(p) = \sum_{p'=0}^{P-1} \sum_{n=0}^{N-1} I(p') \; (y_n(t) * s(-t)|_{t=\tau_{pp'n}}) F(p, p', n), p = 0, \ldots, P-1, \qquad (5)$$

where $\tau_{pp'n}$ is the round-trip path between the transceiver, the first scattering center at $(x_{p'}, z_{p'})$, and the second scattering point at (x_p, z_p). The weighting function $F(p, p', n)$ discards an ellipsoidal region surrounding the line-of-sight between the nth antenna location and the p'th first scattering center to reduce the introduction of ghosts at implausible locations (See the left plot in Fig. 6). Finally, the two images are normalized and superimposed to obtain a composite image, which depicts significantly enhanced visible regions of the targets. For illustration, Fig. 6 also shows the images $I(\cdot)$ and $I^{\text{double}}(\cdot)$ for a scene containing three targets of circular and rectangular shapes. Clearly, the conventional SAR image has difficulty in imaging the sides of the rectangular target, whereas the modified SAR algorithm can reconstruct the rectangular sides of the target. The main advantage of this algorithm is an extension of the visible target region without the need of prior knowledge of the scene distribution or the surrounding environment.

Following a similar idea, the work in [5] proposed a ghost mapping approach, wherein the ghosts in the conventional SAR image, resulting from interior wall multipath, are mapped back onto the respective targets to obtain a ghost-free image with improved SCR. Complete knowledge of the room geometry is assumed, especially the locations of the interior walls. Using this prior knowledge, for any target position, the location of the associated ghosts (one for each interior

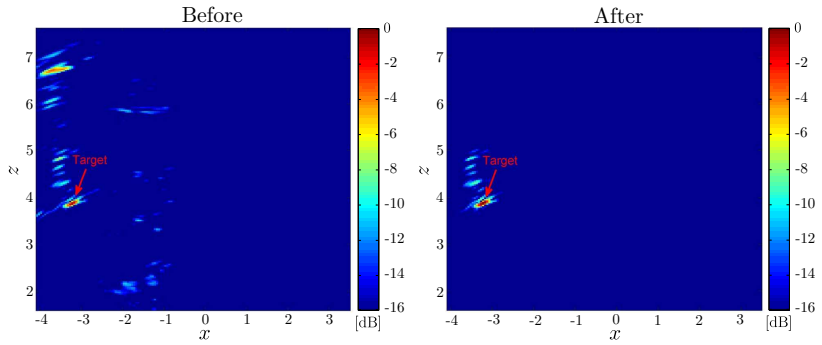

Fig. 7. Backprojected image using the conventional (left) and multipath exploitation based (right) image formation approaches.

wall) can be predicted. The exploitation scheme works as follows. Using conventional image formation, an image of the scene containing both real targets and ghosts is obtained. Next, for every image pixel (and possible target location), the energy of the associated ghosts is mapped back onto the target's site. This is achieved by a 2D convolution with a space-varying kernel $H(p,r)$ that uses the information of the ghost locations

$$I^{\text{mapping}}(p) = \sum_{r=0}^{R-1} |I(p)| * H(p,r). \tag{6}$$

The weighting and shape of the kernel $H(p,r)$ is chosen such that the full energy of the ghosts is utilized to boost the amplitude of the real target. At the same time, the ghosts are suppressed. Finally, a composite ghost-free image with improved SCR is obtained by a pixel-by-pixel multiplication of the two images. Fig. 7 illustrates the result of the multipath exploitation scheme using real data from a scene consisting of a single reflector located between front and back walls. The conventional SAR image (left) shows both the target and the ghost due to multipath, originating from the back wall. The ghost is clearly suppressed in the composite image (right) obtained using the exploitation scheme.

B. Exploitation with Unresolved Multipath

The above described exploitation methods fail if the multipath returns are not resolvable because they would lead to overlapping targets and ghosts in the conventional SAR image. Such situations may arise when system constraints permit use of limited bandwidth and/or aperture, and in the presence of non-homogeneous front walls. However, using proper modeling of the multipath returns, the additional energy and information therein may still be exploited to obtain an improved scene reconstruction.

If prior knowledge of the surrounding environment is available, i.e. the location and dielectric properties of the walls, a linear inverse scattering scheme based on the PO model may be employed for exploiting multipath from walls and other specular reflectors [20]. Using Kirchhoff's approximation, a linearized scattering equation can be obtained as

$$E_s(u_n, k_0) = \iint_{\Omega} E_i(u_n, x, z, k_0) G(u_n, x, z, k_0) \sigma(x, z) dx dz, \tag{7}$$

where $E_s(u_n, k_0)$ is the scattered field measured at the nth antenna location, k_0 is the wave number in free space, $E_i(\cdot)$ is the incident field, $G(\cdot)$ is Green's function for the relevant background medium, $\sigma(x, z)$ is the unknown target distribution, and Ω describes the spatial region being interrogated. With prior knowledge of the background scattering environment, Green's function can be calculated analytically or numerically. The incident field can be obtained by the known emitted field of the transmitter and the reflection/refraction properties of the front wall. Discretizing the region of interest Ω, a finite-dimensional equivalent representation of (7) is obtained as

$$\boldsymbol{E}_s = \boldsymbol{A}_{\text{linscat}} \boldsymbol{\sigma}, \tag{8}$$

where $\boldsymbol{E}_s$ is the vectorized measured scattered field, $\boldsymbol{A}_{\text{linscat}}$ represents the discretized linear operator in (7), and $\boldsymbol{\sigma}$ is the discretized and vectorized scattering space. An estimate of $\boldsymbol{\sigma}$ can be achieved by finding the singular value decomposition of $\boldsymbol{A}_{\text{linscat}}$ and inverting only the dominant singular values [20], [27]. Other inversion methods may employ a sparsifying regularization, as in [21]. Sparse reconstruction based multipath exploitation approaches are described in more detail in Section V.

A similar method has been proposed to deal with multipath resulting from periodically structured front walls, e.g. cinder block walls [4]. The propagation through the front wall is modeled analytically and is exploited in the image formation step to utilize the additional beams that are directed towards the target by the Floquet modes of the front wall.

Time-reversal methods [22]–[24] may also be applied to exploit multipath propagation in indoor imaging. The efficiency of this approach was first demonstrated by Fink [28], using acoustic waves and first applied to multipath environments in SAR by Sarabandi *et al.* [22]. Time reversal is a two-step procedure. In the first step, the pulse is transmitted into the background scene and reflections are received by an array. This is done to obtain information of the scattering scenario without the target of interest. In the second step, a time reversed received signal is transmitted at the receive array into the scene containing the target of interest. In this way, the transmitted

energy is focused at the original transmitter location. By using this scheme, the information of the scattering environment can be used to improve the effective array aperture. It should be noted that if the scattering environment is known *a priori*, the first transmit receive cycle can be executed via a simulation, thereby overcoming the otherwise limiting constraint of background scene access.

V. Multipath Exploitation/Suppression in Sparse Reconstructions

Sparse signal representation has been used successfully for solving SAR image formation problems in a variety of applications [29]. This framework is based on the observation that typical underlying scenes usually exhibit sparsity in terms of certain features, such as scene reflectivity.

Sparse representation was first employed for imaging of building interiors in [30]. As only a few targets usually reside in the room, the complex amplitude of the image can be sparsely represented. The measurement model, motivated by the ray-tracing formulation of (1), is given by

$$\boldsymbol{y} = \boldsymbol{A}\boldsymbol{\sigma}, \tag{9}$$

where $\boldsymbol{y}$ is the stacked vector representing the measurements from all N array element locations, $\boldsymbol{\sigma}$ is the sparse vectorized image of the scene, and the matrix $\boldsymbol{A}$ is the dictionary of the radar responses under the assumed single-scattering based point-target model. The scene image can be reconstructed using the basis pursuit denoising (BPDN) as follows

$$\hat{\boldsymbol{\sigma}} = \min_{\boldsymbol{\sigma}} \frac{1}{2}\|\boldsymbol{A}\boldsymbol{\sigma} - \boldsymbol{y}\|_2^2 + \lambda\|\boldsymbol{\sigma}\|_1, \tag{10}$$

where λ is a regularization parameter which provides a trade-off between fidelity to measurements and noise tolerance. BPDN is a regularized least-squares solution that favors sparse results. Other reconstruction methods use greedy approaches to build the solution iteratively. Optionally, a downsampling of the measurements in (9) can be done to reduce the amount of data. However, special care has to be taken to ensure incoherence of the sampling matrix and the dictionary in order to guarantee reliable recovery.

The sparse reconstruction approach for indoor images has been extended to exploit both interior wall and wall ringing multipath returns in [19] under the assumption of prior knowledge of building layout. Using a discretized version of the ray-tracing signal model in (2) and assuming knowledge of the building layout, the measurement vector $\boldsymbol{y}$ can be expressed as a superposition of individual linear models for each of the R propagation paths

$$\boldsymbol{y} = \boldsymbol{A}^{(0)}\boldsymbol{\sigma}^{(0)} + \boldsymbol{A}^{(1)}\boldsymbol{\sigma}^{(1)} + \cdots + \boldsymbol{A}^{(R-1)}\boldsymbol{\sigma}^{(R-1)}, \tag{11}$$

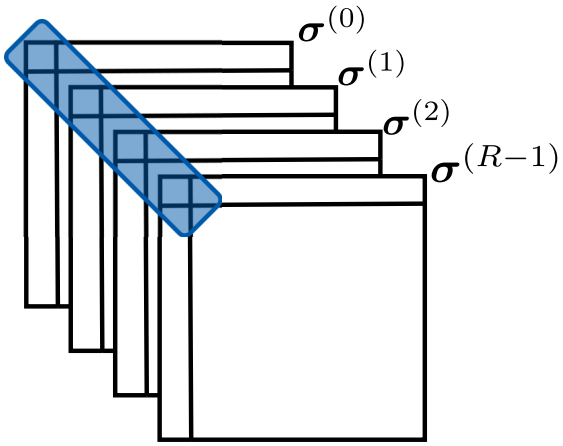

Fig. 8. Group sparse structure for the sub-images.

where $\boldsymbol{\sigma}^{(r)}$ is the vectorized image of the scene corresponding to the rth path and $\boldsymbol{A}^{(r)}$ is the dictionary that embodies the GO propagation model for the rth path. Next, a stacked signal model is formed

$$\boldsymbol{y} = \tilde{\boldsymbol{A}}\tilde{\boldsymbol{\sigma}}, \tag{12}$$

with a combined dictionary $\tilde{\boldsymbol{A}} = [\boldsymbol{A}^{(0)} \ \boldsymbol{A}^{(1)} \ \cdots \ \boldsymbol{A}^{(R-1)}]$ and stacked image vectors $\tilde{\boldsymbol{\sigma}} = \left[\left(\boldsymbol{\sigma}^{(0)}\right)^T \ \left(\boldsymbol{\sigma}^{(1)}\right)^T \ \cdots \ \left(\boldsymbol{\sigma}^{(R-1)}\right)^T\right]^T$. The vector $\tilde{\boldsymbol{\sigma}}$ can be estimated by exploiting the common support property of the R sparse images. This property stems from the fact that the images $\boldsymbol{\sigma}^{(0)}, \ldots, \boldsymbol{\sigma}^{(R-1)}$ describe the same underlying scene. That is, if a certain element in, e.g., $\boldsymbol{\sigma}^{(0)}$ has a nonzero value, the corresponding elements in the other images should be also nonzero. This means that corresponding pixels in the image vectors should be grouped, as shown in Fig. 8, necessitating a group sparse reconstruction approach

$$\hat{\tilde{\boldsymbol{\sigma}}} = \arg\min_{\tilde{\boldsymbol{\sigma}}} \frac{1}{2}\|\bar{\boldsymbol{y}} - \tilde{\boldsymbol{A}}\tilde{\boldsymbol{\sigma}}\|_2^2 + \lambda\|\tilde{\boldsymbol{\sigma}}\|_{2,1}, \tag{13}$$

where

$$\begin{aligned}\|\tilde{\boldsymbol{\sigma}}\|_{2,1} :&= \sum_{p=0}^{P-1} \left\| \left[\sigma_p^{(0)}, \sigma_p^{(1)}, \ldots, \sigma_p^{(R-1)}\right]^T \right\|_2 \\ &= \sum_{p=0}^{P-1} \sqrt{\sum_{r=0}^{R-1} \sigma_p^{(r)} \left(\sigma_p^{(r)}\right)^*}.\end{aligned} \tag{14}$$

The mixed-norm term in the regularizer ensures the group structure in the sparse reconstruction result. Finally, the reconstruction results for the individual paths are combined non-coherently to obtain an overall image with suppressed ghost targets and improved SCR, see Fig. 9. Data undersampling can precede the sparse reconstruction in this approach as well.

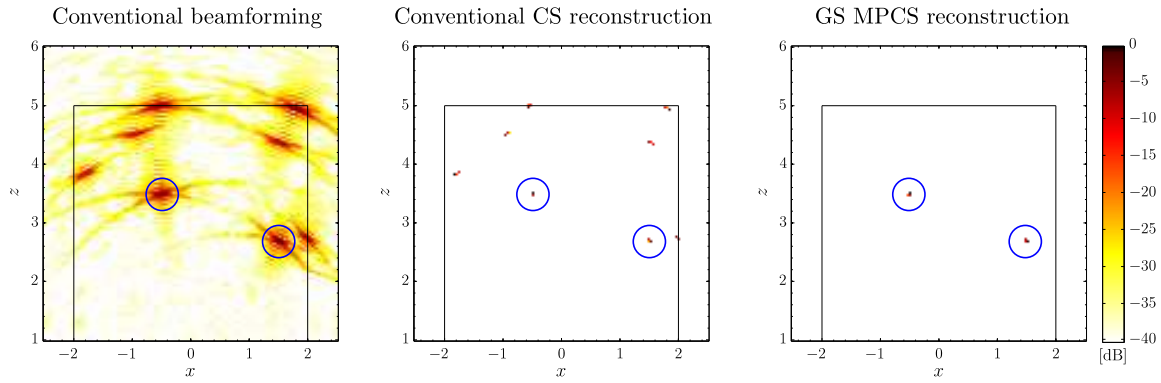

Fig. 9. Backprojected image using the full data (left), along with conventional (center) and multipath exploitation based (right) sparse reconstruction results. The sparse reconstruction used undersampled data, specifically, one fourth of the array elements and on eighth of the frequencies.

An alternate approach for sparsity based scene reconstruction in the presence of multipath has been proposed in [16]. The authors assume a convolutive model for multipath, wherein the echo waveform at each receiver is modeled as the superposition of the direct impulse response and the multipath impulse response for P targets convolved with the transmitted pulse waveform $\boldsymbol{s}$

$$\boldsymbol{y}_p = \sum_{p=0}^{P-1} \boldsymbol{s} * (\boldsymbol{g}_p + \boldsymbol{d}_p * \boldsymbol{g}_p). \tag{15}$$

The direct impulse response $\boldsymbol{g}_p$ is assumed to be a single spike and stronger than the indirect returns. The multipath impulse response is the convolution of the direct impulse response $\boldsymbol{g}_p$ with a sparse delay vector $\boldsymbol{d}_p$. The multipath delays for a particular target are assumed constant across the receivers. Using the above model, an iterative greedy sparse reconstruction approach is proposed by the authors to estimate the unknown impulse responses $\boldsymbol{g}_p$ and delay vectors $\boldsymbol{d}_p$. The estimated direct impulse responses are then used to form a ghost-free image. The method performs well, especially in the case of wall ringing multipath. The advantage of this approach lies in the fact that no prior knowledge is needed. However, the additional energy in the multipath returns is suppressed rather than exploited for image formation.

VI. Conclusion

We have considered the problem of imaging building interiors using sythetic aperture radar. The emerging TWRI technology has experienced a rising interest over the last decade due to its numerous civil and military applications. We have presented an overview of different approaches to deal with multipath in indoor radar imaging scenarios. Multipath mitigation and exploitation are

key to obtaining reliable information when many and/or strong secondary scatterers are present in the scene of interest. We have provided a balanced and complete account of existing methods and discussed their respective advantages and disadvantages. Both conventional beamforming and compressive sensing based methods have been presented, where the latter assume the underlying scene to be sparse. We bridged analysis with supporting simulation and experimental examples.

REFERENCES

[1] M. Amin and F. Ahmad, "Wideband synthetic aperture beamforming for through-the-wall imaging [lecture notes]," *IEEE Signal Processing Magazine*, vol. 25, no. 4, pp. 110–113, July 2008.

[2] M. Amin, Ed., *Through-the-Wall Radar Imaging*. CRC Press, 2010.

[3] T. Dogaru and C. Le, "SAR images of rooms and buildings based on FDTD computer models," *IEEE Transactions on Geoscience and Remote Sensing*, vol. 47, no. 5, pp. 1388–1401, May 2009.

[4] R. Burkholder, "Electromagnetic models for exploiting multi-path propagation in through-wall radar imaging," in *Int. Conf. on Electromagnetics in Advanced Applications*, Torino, Italy, Sep. 2009, pp. 572–575.

[5] P. Setlur, M. Amin, and F. Ahmad, "Multipath model and exploitation in through-the-wall and urban radar sensing," *IEEE Transactions on Geoscience and Remote Sensing*, vol. 49, no. 10, pp. 4021–4034, Oct. 2011.

[6] E. J. Baranoski, "Multipath exploitation radar industry day," DARPA. Herndon, VA, 2007.

[7] W. Liang, H. Xiaotao, Z. Zhimin, and S. Qian, "Research on UWB SAR image formation with suppressing multipath ghosts," in *CIE Int. Conf. on Radar*, Shanghai, China, Oct. 2006, pp. 1–3.

[8] Q. Tan and Y. Song, "A new method for multipath interference suppression in through-the-wall UWB radar imaging," in *Int. Conf. on Advanced Computer Control (ICACC)*, vol. 5, Shenyang, China, March 2010, pp. 535–540.

[9] D. Garren, "SAR image formation uncorrupted by multiple-bounce artifacts," in *IEEE Radar Conf.*, Long Beach, USA, April 2002, pp. 338–343.

[10] D. Obuchon, D. Garren, J. S. Goldstein, R. Greene, and J. North, "Drift inversion estimation of multipath ghosts in sar image reconstruction," in *IEEE Radar Conf.*, Philadelphia, USA, April 2004, pp. 556–558.

[11] J. DeLaurentis, "Multipath synthetic aperture radar imaging," *IET Radar, Sonar Navigation*, vol. 5, no. 5, pp. 561–572, Jun. 2011.

[12] F. Ahmad and M. Amin, "Multi-location wideband synthetic aperture imaging for urban sensing applications," *Journal of the Franklin Institute*, vol. 345, no. 6, pp. 618–639, Sept. 2008.

[13] L. Li and J. Krolik, "Vehicular MIMO SAR imaging in multipath environments," in *IEEE Radar Conf.*, Kansas City, USA, May 2011, pp. 989–994.

[14] D. B. André, R. D. Hill, and C. P. Moate, "Multipath simulation and removal from SAR imagery," in *Proc. SPIE 6970, Algorithms for Synthetic Aperture Radar Imagery XV*, April 2008, p. 69700M.

[15] A. O. Knapskog, "Moving targets and multipath in sar images of harbour scenes," in *European Conf. on Synthetic Aperture Radar (EUSAR)*, Nuremberg, Germany, April 2012, pp. 547–550.

[16] H. Mansour and D. Liu, "Blind multi-path elimination by sparse inversion in through-the-wall-imaging," in *IEEE Int. Workshop on Computational Advances in Multi-Sensor Adaptive Processing (CAMSAP)*, Saint Martin, Dec. 2013.

[17] R. Price and P. Green, "A communication technique for multipath channels," *Proc. IRE*, vol. 46, no. 3, pp. 555–570, Mar. 1958.

[18] S. Kidera, T. Sakamoto, and T. Sato, "Extended imaging algorithm based on aperture synthesis with double-scattered waves for UWB radars," *IEEE Transactions on Geoscience and Remote Sensing*, vol. 49, no. 12, pp. 5128–5139, Dec. 2011.

[19] M. Leigsnering, F. Ahmad, M. Amin, and A. Zoubir, "Multipath exploitation in through-the-wall radar imaging using sparse reconstruction," *IEEE Transactions on Aerospace and Electronic Systems*, 2013, in press.

[20] G. Gennarelli and F. Soldovieri, "A linear inverse scattering algorithm for radar imaging in multipath environments," *IEEE Geoscience and Remote Sensing Letters*, vol. 10, no. 5, pp. 1085–1089, Sept. 2013.

[21] G. Gennarelli, I. Catapano, and F. Soldovieri, "RF/microwave imaging of sparse targets in urban areas," *IEEE Antennas Wireless Propagation Letters*, vol. 12, pp. 643–646, May 2013.

[22] K. Sarabandi, I. Koh, and M. Casciato, "Demonstration of time reversal methods in a multi-path environment," in *IEEE Antennas and Propagation Society International Symposium*, vol. 4, Monterey, USA, June 2004, pp. 4436–4439.

[23] J. M. F. Moura and Y. Jin, "Time reversal imaging by adaptive interference canceling," *IEEE Transactions on Signal Processing*, vol. 56, no. 1, pp. 233–247, Jan. 2008.

[24] W. Zheng, Z. Zhao, and Z.-P. Nie, "Application of TRM in the UWB through wall radar," *Progress In Electromagnetics Research*, vol. 87, pp. 279–296, 2008.

[25] K. J. Langenberg, M. Brandfaß, K. Mayer, T. Kreutter, A. Brüll, P. Fellinger, and D. Huo, "Principles of microwave imaging and inverse scattering," *EARSeL advances in remote sensing*, vol. 2, no. 1, pp. 163–186, 1993.

[26] F. Soldovieri and R. Solimene, "Through-wall imaging via a linear inverse scattering algorithm," *IEEE Geoscience and Remote Sensing Letters*, vol. 4, no. 4, pp. 513–517, 2007.

[27] R. Solimene, F. Soldovieri, G. Prisco, and R. Pierri, "Three-dimensional through-wall imaging under ambiguous wall parameters," *IEEE Transactions on Geoscience and Remote Sensing*, vol. 47, no. 5, pp. 1310–1317, March 2009.

[28] M. Fink, "Time-reversal mirrors," *Journal of Physics D: Applied Physics*, vol. 26, no. 9, p. 1333, 1993.

[29] L. Potter, E. Ertin, J. Parker, and M. Cetin, "Sparsity and compressed sensing in radar imaging," *Proc. of the IEEE*, vol. 98, no. 6, pp. 1006–1020, June 2010.

[30] Y.-S. Yoon and M. Amin, "Compressed sensing technique for high-resolution radar imaging," in *Proc. of SPIE Signal Processing, Sensor Fusion, and Target Recognition XVII*, vol. 6968, no. 1, Orlando, USA, March 2008, p. 69681A.

Michael Leigsnering received the Dipl.-Ing. degree in electrical engineering and information technology with summa cum laude from Technische Universität Darmstadt in 2010. He is currently working towards his Ph.D. degree in the Signal Processing Group, Institute of Telecommunications, Technische Universität Darmstadt. His research interest lies in array signal processing with focus on through-the-wall radar imaging, compressive sensing, and multipath phenomena. He has been a visiting research associate at the Center for Advanced Communications, Villanova University, Villanova, PA in 2012 and 2013.

Moeness G. Amin received his Ph.D. degree in 1984 from University of Colorado, Boulder. He has been on the Faculty of the Department of Electrical and Computer Engineering at Villanova University since 1985, where he is now a Professor and the Director of the Center for Advanced Communications. Dr. Amin is a Fellow of IEEE, SPIE, and IET. He is a Recipient of the IEEE Third Millennium Medal and EURASIP Individual Technical Achievement Award. He was a Distinguished Lecturer of the IEEE Signal Processing Society. Dr. Amin has over 600 publications in the field of signal and array processing, including radar imaging. He is a recipient of eight best paper awards. He serves on the IEEE Signal Processing Magazine and Signal Processing Journal Editorial Boards.

Fauzia Ahmad received her M.S. and Ph.D. degrees in electrical engineering, both from the University of Pennsylvania, Philadelphia, in 1996 and 1997, respectively. Since 2002, she has been with the Center for Advanced Communications, Villanova University, Villanova, PA, where she is now a Research Professor and the Director of the Radar Imaging Lab. She has over 130 publications in the areas of radar imaging, radar signal processing, compressive sensing, array signal processing, waveform design and diversity, ultrasound imaging, and over-the-horizon radar. Dr. Ahmad is a senior member of IEEE and SPIE. She serves on the editorial boards of the IET Radar, Sonar, and Navigation Journal and the SPIE/IS&T Journal of Electronic Imaging.

Abdelhak M. Zoubir received his Dr.-Ing. degree from Ruhr-Universität Bochum, Germany. He was with Queensland University of Technology, Australia, from 1992 to 1998. He then joined Curtin University of Technology, Australia, as a Professor of Telecommunications and was interim Head of the School of Electrical and Computer Engineering from 2001 to 2003. Since 2003, he has been a Professor of Signal Processing at Technische Universität Darmstadt, Germany. He is a Fellow of IEEE, an IEEE Distinguished Lecturer (Class of 2010–2011), Past-Chair of the Signal Processing Theory and Methods Technical Committee of the IEEE Signal Processing Society, and currently the Editor-in-Chief of the IEEE Signal Processing Magazine. His research interest lies in statistical methods for signal processing applied to telecommunications, radar, sonar, car engine monitoring, and biomedicine. He has published over 300 papers in these areas.